Dual Cage High Power Induction Motor with Direct Start-up. Design and FEM Analysis

Leonard LIVADARU, Alecsandru SIMION, Adrian MUNTEANU, Margareta COJAN, Ovidiu DABIJA
Gheorghe Asachi Technical University of Iaşi, 700050, Romania
livadaru@ee.tuiasi.ro

***Abstract*—This paper presents an investigation on the design of high-power induction motor with special constraints. Direct online start-up and pull-up torque of rather high value represent two of the imposed requirements. Three different structures are analyzed, which involve deep bars, magnetic wedges and double cage respectively. The proposed solution advances a new rotor structure with two different rotor cages. The first cage acts mainly during start-up and is made of iron with both electric and magnetic properties. The second one is made of copper and represents the main rotor winding. It has a particular cross-section of the bars in order to carry into effect the required constraints both during start-up and steady-state. The proposed models are finally evaluated by means of finite element method analysis.**

***Index Terms*—direct start-up, dual cage, finite element analysis, high-power induction motor, magnetic wedges.**

I. INTRODUCTION

It is a fact that the new trend in electric drives is to use electric motors that are particularly designed for a certain application. Often, the constraints that have to be fulfilled are somehow contradictory and do not match to performance criteria. Obviously, such cases represent a real challenge for the designer.

In this paper such a case is presented. It is about the design of a high-power induction motor destined to mining industry. The rated input/output quantities are presented in Table I.

TABLE I. NOMINAL PARAMETERS

Parameter	Value
Supply voltage, U_1 – Y connection	6 kV
Supply frequency, f_1	50 Hz
Output power, P_2	630 kW
Number of pole pairs, p	2

More important for the design of the machine are the start-up conditions. The three-phase motor is going to be direct connected to the mains and the ratio starting-current/nominal-current must be less than 3 ($I_s/I_n < 3$). Additionally, the pull-up torque must be higher than the nominal torque ($T_s/T_n > 1$) and the pull-out torque has to be 1.4 times greater than nominal torque ($T_{max}/T_n > 1.4$). And finally, the nominal current must not exceed a value of 90 A.

Taking into consideration the above mentioned requests, we present in this paper three design solutions.

II. DESIGN SOLUTIONS

The basic preliminary analysis put in view two major issues that have to be accomplished: low starting current and high starting torque. These are two opposite requests, which eventually can be obtained with a special structure of the machine.

The design procedure took into consideration three solutions which could provide the start-up constraints: deep bars, magnetic wedges and double cage. Both deep bars and double cage structures [1-4] have the same effects that are decrease of the starting current and increase of the pull-up torque. Unfortunately, the decrease of the starting current is usually limited to at the very most $4.5I_n$, which is nothing less than insufficient. The magnetic wedges, on the other hand, are generally placed in stator slots and they usually bring maximum of 20% of current reduction both for start-up or steady-state operation [5-14].

A few preliminary simulations guided us in considering three possible solutions, which could fulfill the operation requirements. For each of them, the rotor structure and more precisely the rotor winding is the subject of modification, while the stator structure stands unchanged.

The first solution refers to a *deep bar copper* rotor winding, Fig.1 and Fig. 2, [15], [16]. Additionally, the shape of the bars has two rectangular areas of different cross-sections, which are connected by a narrow duct [17], [18]. As a matter of fact, the shape tells of the regular double cage structure and satisfies two requirements. The diminished cross-section of the bar leads to an increased resistance and the free space allows a supplementary ventilation of the bars (the machine is provided with forced ventilation). From reasons that belong with a proper comparison, the position of the bars is deeper inside the rotor and the upper part of the rotor slots hosts, for example, insulating material (simulations with bars that are placed next to the air-gap proved no superior results).

The second solution adds iron bars (Fig. 1 and Fig. 2), which are placed in the rotor slots in the place of rectangular insulation. These bars act as *magnetic wedges* and have both magnetic and electric properties. The magnetization curve corresponds to regular steel (inferior values up against laminations of the magnetic circuit) and the electric resistivity is of $\rho=1.8\cdot10^{-7}\Omega m$ ($\rho_{Cu20}=1.7\cdot10^{-8}\Omega m$ – for comparison).

The third solution transforms the magnetic wedges into a second rotor cage. As it will be proven, this iron cage plays a major role during start-up and acts insignificant during steady-state operation.

Fig. 1 shows a 3D close-up view of the stator and rotor slots and Fig. 2 presents in a 2D view more information concerning the dimensions of the slots. As regards the main geometrical parameters of the motor, they are presented in Table II.

Digital Object Identifier 10.4316/AECE.2013.02009

TABLE II. MAIN GEOMETRICAL PARAMETERS

Parameter	Value
Inner stator diameter	0.56 m
Outer stator diameter	0.84 m
Air-gap width	1.5 mm
Inner rotor diameter	0.3 m
Axial length of magnetic circuit (9 stacks separated by radial air-gaps of 10mm)	0.57 m
Stator slots number	54
Rotor slots number	64
Number of turns/stator slot (rectangular type)	24

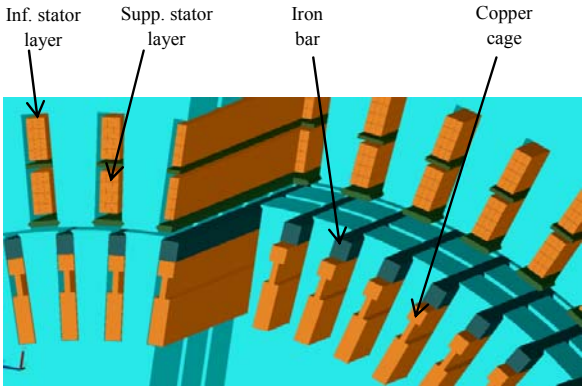

Figure 1. 3D close-up view

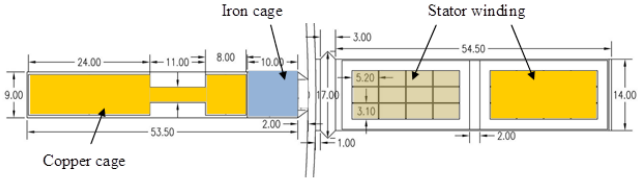

Figure 2. 2D view of stator and rotor slots

III. Performance Evaluation by Finite Element Analysis

The use of the finite element method in design of electrical machines became a needful tool since it provides exact information concerning electric and magnetic quantities for every point of the machine [19], [20]. The simulation presented in this paper have used Flux2D software package from CEDRAT. It has been performed a magnetodynamic analysis, which characterizes the steady-state operation of the motor.

By means of iterative processing method, one can obtain the most important characteristics of the motor which are torque/slip variation (Fig. 3) and current/slip variation (Fig. 4) for the three proposed solutions. The differences are significant and corresponds mainly to unsteady operation segments (start towards nominal). Table III points out the values of the requested parameters and Table IV presents the requested ratios.

It is worth to make some remarks. The single cage solution ensures a high T_{max}/T_n ratio but the I_s/I_n ratio is too high as well. Then the starting torque is completely insufficient up against the requests.

The presence of the magnetic wedges brings a strong decrease of the starting current but the pull-up torque decreases dramatically and the pull-out torque remains too small.

The transformation of the magnetic wedges into a second cage brings the machine very close to requested parameters. Both T_{max}/T_n and I_s/I_n ratios can be considered as accomplished demands and the T_s/T_n ratio finally fulfill the imposed requirement. From this point of view, we can consider that the *double cage* rotor represents the solution which solves the requested demands.

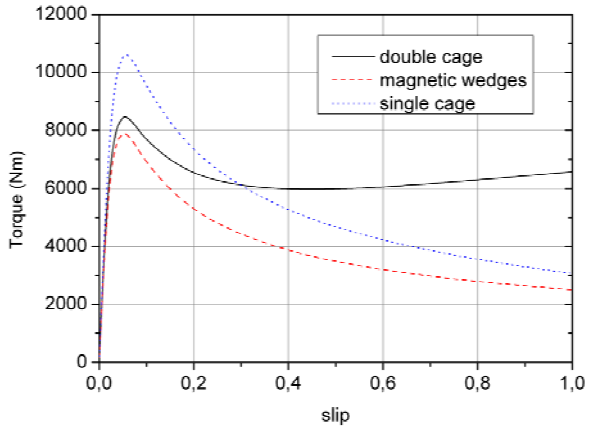

Figure 3. Torque-slip characteristic, T=f(s)

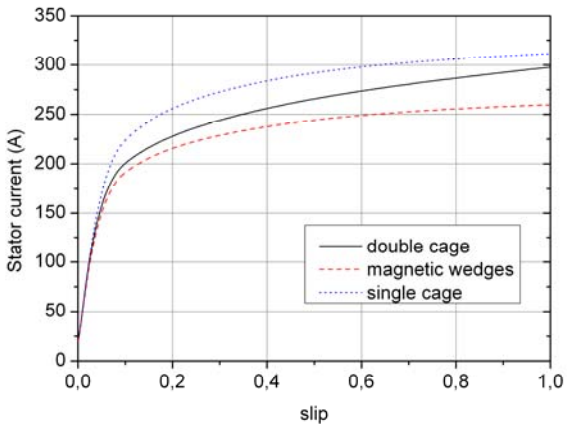

Figure 4. Current-slip characteristic, I=f(s)

TABLE III. TORQUE AND CURRENT SPECIFIC VALUES

	Pull-up torque, Ts	Pull-out torque, Tmax	Starting current, Is	Nominal current, In	Nominal slip, s	Nominal torque, Tn
Double cage	6571 Nm	8471 Nm	298 A	91 A	0.021	6260 Nm
Magnetic wedges	2506 Nm	7900 Nm	260 A	93 A	0.023	6272 Nm
Single cage	3070 Nm	10614 Nm	311 A	78 A	0.017	6234 Nm

TABLE IV. REQUESTED PARAMETERS RATIOS

Structure	Ts/Tn	Tmax/Tn	Is/In
Double cage	1.05	1.35	3.27
Magnetic wedges	0.4	1.26	2.8
Single cage	0.49	1.7	3.99
Initial requested values	> 1	> 1.4	< 3

Fig. 5 presents the flux density color maps corresponding to nominal point operation for each structure. It is interesting to notice that the iron bars and small areas of rotor teeth are the subject of saturation. They represent sensitive areas of the machine which needs special

ventilation due to increased iron losses and expectable heating.

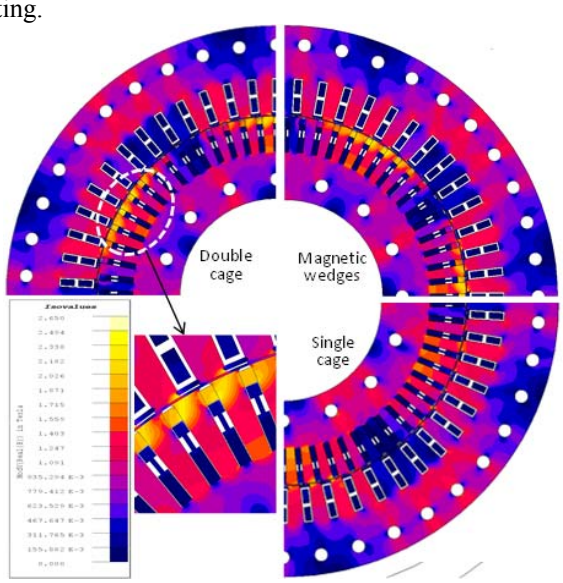

Figure 5. Flux density color map

Another parameter that has to be verified is the current density. Fig. 6 (nominal operation) and Fig. 7 (start-up) show color maps of the distribution of this quantity. On one hand, it has to be pointed out that under nominal operation the current density value is slightly higher than usual recommended values (7.6 A/mm^2 in stator winding and 5.5 A/mm^2 in rotor bars). However these are not alarming rates but again, forced ventilation is necessary. On the other hand, the iron bars have poor (double cage structure) and insignificant (magnetic wedges structure) values of current density. The color maps (Fig. 7) of the current density corresponding to start-up prove the presence of the skin effect in copper bars and show mainly for the double cage structure the participation of the iron bars to the start-up process.

As regards the air-gap flux density wave (Fig. 8), there are certain differences between the single cage structure and the two others which are better pointed out by the Fourier analysis and content in high order harmonics (Fig. 9). The most significant is the 17th harmonic but the 5th harmonic is unusual high despite the short-pitch stator winding.

Finally, Fig. 10 presents the efficiency and power factor characteristics corresponding to the *double cage* structure, which was selected as the viable solution. If the efficiency value is quite good ($\eta = 0.92$), the power factor has a low value ($\cos \varphi = 0.74$) mainly due to the presence of the iron-cage.

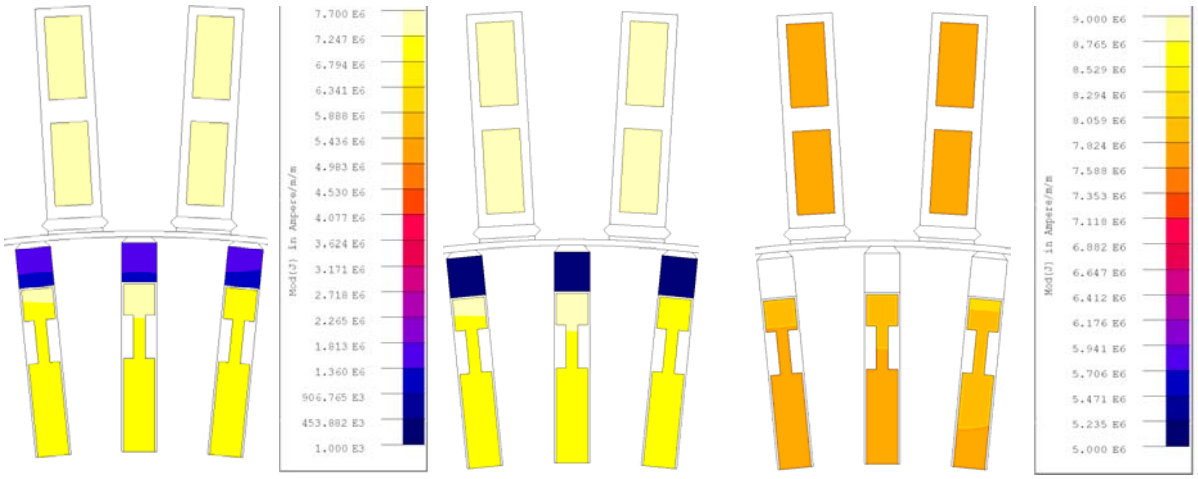

Figure 6. Current density color maps – nominal operation

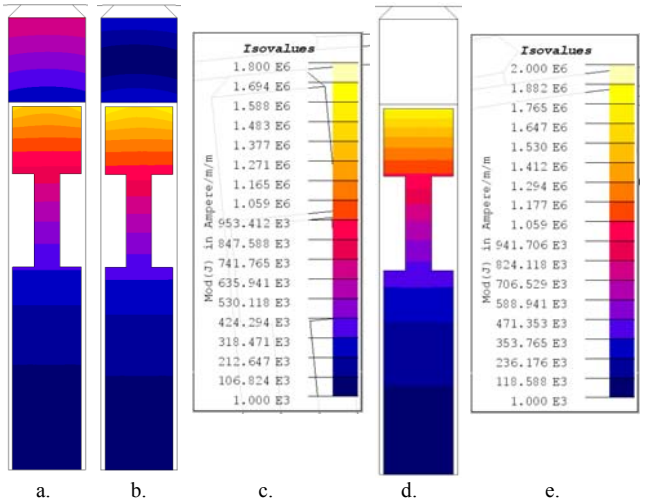

Figure 7. Current density color maps – start-up: a-double cage, b-magnetic wedges, c. Legend for a and b, d-Single cage, e-Legend for d

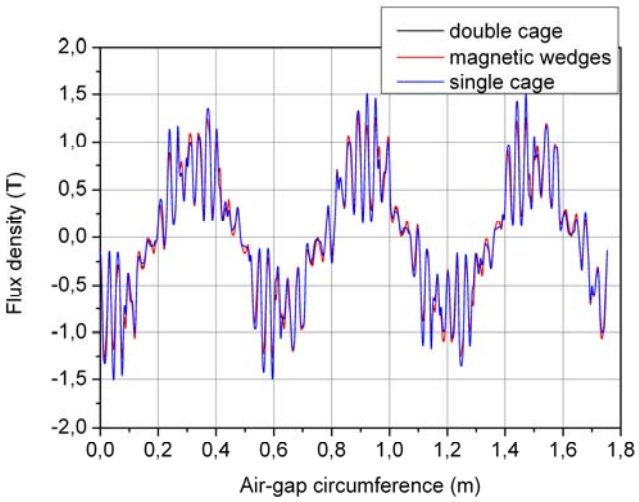

Figure 8. Air-gap flux density wave

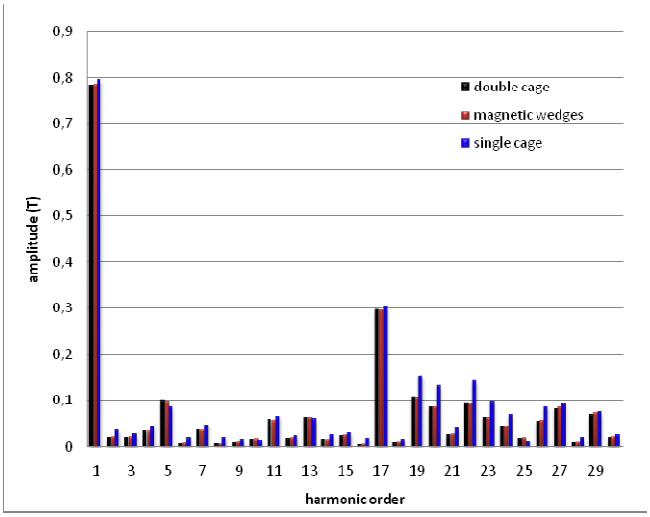

Figure 9. Content in high order harmonics

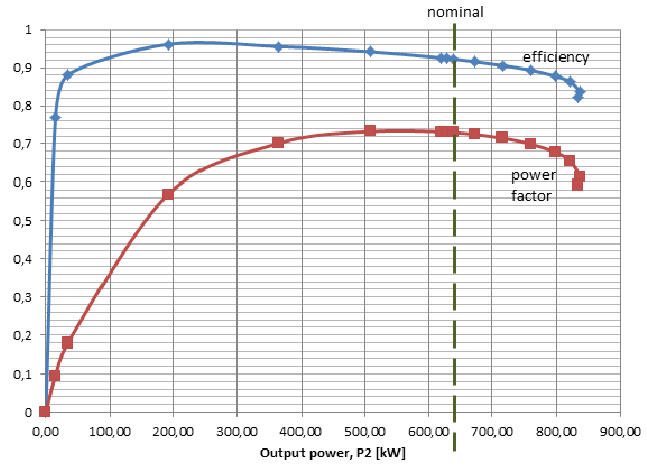

Figure 10. Efficiency and power factor

IV. Conclusion

The paper presents the design and evaluation procedure for a three-phase high power induction motor with severe start-up constraints. The most unusual request is the direct online start-up, which implies a low starting current value ($I_s/I_n<3$). Additionally, the electric drive needs both a high starting torque ($T_s/T_n>1$) and a reasonable pull-out torque ($T_{max}/T_n>1.4$). No doubt, the requirements are somehow contradictory and ask for a special structure. The proposed solution implies the presence of two distinct rotor cages made of different materials, copper and iron.

The main cage (the copper one), which is a deep bar structure, acts both on start-up and regular under-load operation. It concurs to the decrease of the starting current and increase of the starting torque. But its influence cannot reach by itself the imposed requests. There is insufficient decrease of the current and the pull-up torque does not increase as demanded.

The presence of iron bars placed in rotor slots is so very significant. When they act as magnetic wedges there is a strong decrease of the starting current but the value of the pull-up torque decreases, as well. The solution is to transform the magnetic wedges into a second iron cage, which acts mainly during start-up. Thus, the increased total resistance of the rotor winding leads to a decrease of the starting current and increase of the pull-up torque. For this purpose, the iron material of the bars must have both magnetic and electric properties.

One more remark has to be mentioned. The severe constraints imposed for the motor operation ask for a special design where the value of the electromagnetic loads goes toward upper limits and beyond them. It is mandatory the use of superior materials (for example high quality ferromagnetic laminations) and the presence of supplementary (forced) ventilation.

References

[1] I. Boldea, S. Nasar. The Induction Machines Design Handbook, CRC Press, 2010.

[2] J. Pyrhonen, T. Jokinen, V. Hrabovkova. Design of rotating electrical machines, Wiley & Sons, 2008.

[3] K. Gyftakis, J. Kappatou, A. Safacas, "FEM study of asynchronous cage motors combining NEMA's classes A and D slot geometry". In Proc. of ICEM 2010, Rome, pp. 1-6, 6-8 Sept. 2010.

[4] K. Gyftakis, D. Athanasopoulos, J. Kappatou, "Study of double cage induction motors with different rotor bar materials", In Proc. of ICEM 2012, Marseille, pp. 1450-1456, 2-5 Sept. 2012.

[5] R. Hanna, W. Hiscock, P. Klinovski, **"**Failure Analysis of Three Slow-Speed Induction Motors for Reciprocating Load Application". IEEE Trans Ind. Applic., Vol.43, No.2, pp. 429-435, March/April 2007.

[6] R. Curiac, H. Li, "Improvements in Energy Efficiency of Induction Motors by the Use of Magnetic Wedges", In Proc. of Petroleum and Chemical Industry Conference (PCIC 2011), Toronto, pp. 1-6, 19-21 Sept. 2011.

[7] Gh. Madescu, M. Greconici, M. Biriescu, M. Moţ, "Effects of stator slot magnetic wedges on the induction motor performances", In Proc. of OPTIM 2012 Conference, Braşov, pp. 489-492, 24-26 May 2012.

[8] J. Kappatou, K. Gyftakis, A. Safacas, "A study of the effects of the stator slots wedges material on the behavior of an induction machine", In Proc. of ICEM 2008, Vilamoura, pp. 1-6, 6-9 Sept. 2010.

[9] Z. Milojkovic, D. Ban, M. Petrinic, J. Studiz, Z. Maljkovic, J. Polak, "Application of Magnetic Wedges for Stator Slots of Hydrogenerators", In Proc. of CIGRE 2010, Paris, 2010. [Online]. Available: http://bib.irb.hr/datoteka/481722.A1_101_2010.pdf

[10] M. Dems, K. Komeza, J.K. Sykulski, "Analysis of Effects of Magnetic Slot Wedges on Characteristics of Large Induction Motors", In Proc. of ISEF 2011, Funchal, 2011. [Online]. Available: http://eprints.soton.ac.uk/272763/

[11] D. Meng, B. Li, Y. Xia, "Calculation and Analysis of Magnetic Slot Wedge Impact on Performance of Medium-Size Motors with High-Voltage", Journal of Computation and Theoretical Nanoscience, Vol.9, Nr.10, pp. 1782-1786, Oct. 2012.

[12] J.F. Gieras, J. Saari, "Performance calculation for a high speed solid-rotor induction motor", In Proc. of IECON 2010, Glandale, pp. 1748-1753, 7-10 Nov. 2010.

[13] J. Pyrhonen, J. Nerg, P. Kurronen, U. Lauber, "High-speed, 8MW, solid-rotor induction motor for gas compression", In Proc. of ICEM 2008, Vilamoura, pp. 1-6, 6-9 Sept. 2010.

[14] Y. Gessese, A. Binder, "Axially slitted, high- speed solid-rotor induction motor technology with copper end-rings", In Proc. of ICEMS 2009, Tokyo, pp. 1-6, 15-18 Nov. 2009.

[15] K.J. Park, K. Kim, S. Lee, D.-H. Koo, K.-C. Koo, J. Lee, "Optimal Design of rotor slot of three-phase induction motor with die-cast copper rotor cage", In Proc. of ICEMS 2008, Wuhan, pp. 61-63, 17-20 Oct. 2008.

[16] T. Tudorache, L. Melcescu, "FEM Optimal Design of Energy Efficient Induction Machines". Advances in Electrical and Computer Engineering, Vol.9, Iss.2, pp. 58-64, Jun. 2009.

[17] V. Fireţeanu, T. Tudorache, O.A. Turcanu, "Optimal Design of Rotor Slot Geometry of Squirrel Type Induction Motors", In Proc. of IEMDC'07, Antalya, Turkey, pp. 537-542, 3-5 May 2007.

[18] S. Sal, L.T. Ergene, "Analysis of the rotor bar geometry's effect on the induction motor performance with finite element method", In Proc. of ELECO 2010, Bursa, Turkey, pp. 320-324, 2-5 Dec. 2010.

[19] N. Bianchi. Electrical machine analysis using finite elements, Taylor&Francis, 2005.

[20] G. Meunier. The finite element method for electromagnetic modeling, Wiley & Sons, 2008.